2010

Small Molecule Inhibitors of MAPK and PI3K Pathways Enhance MDA-7 Lethality in Renal Cell Carcinoma

Patrick Eulitt
Virginia Commonwealth University

Small Molecule Inhibitors of MAPK and PI3K Pathways Enhance MDA-7 Lethality in Renal Cell Carcinoma

A thesis submitted in partial fulfillment of the requirements for the degree of Master of Science at Virginia Commonwealth University

By:

Patrick Eulitt
Bachelor of Arts
Wake Forest University
Winston-Salem, North Carolina 2008

Director: Paul Dent Ph.D.,
Vice Chair of Research, Neuro-Oncology

Virginia Commonwealth University
Richmond, Virginia
April, 2010

ACKNOWLEDGEMENT

I would like to thank my family for their support throughout my education. I would also like to thank all members of the Dent lab, including Dr. Margaret Park, Dr. Clint Mitchell, Hossein Hamed, and Dr. Teneille Walker for their knowledge and patience throughout my research project. I am especially grateful for my committee members for mentoring me over the past year: Dr. De Felice for his continual support and encouragement since the day we first met, Dr. Adly Yacoub for answering my endless questions, and Dr. Paul Dent for the opportunity to learn and work in his lab for the past year.

TABLE OF CONTENTS

LIST OF TABLES

Table…….....Page

LIST OF FIGURES

Figure…….. .....Page

LIST OF ABBREVIATIONS

Full Name	Abbreviation
Activating Transcription Factor	ATF
Adenovirus	Ad.
AKT8 Virgus Oncogene Cellular Homolog	AKT
Ammonium Persulfate	AP
Analysis of Variance	ANOVA
Apoptosis Signal-regulating Kinase 1	ASK1
Apoptotic protease activating factor 1	Apaf-1
B-cell lymphoma 2	BCL-2
B-cell lymphoma extra large	BCL-XL
B-cell lymphoma 2-associated death promoter	BAD
B-cell lymphoma 2-associated X protein	BAX
B-cell lymphoma 2 homologous antagonist killer	BAK
c-Jun NH_2-terminal Kinase	JNK
CCAAT/enhancer Binding Protein	CHOP
Coxsackievirus and Adenovirus Receptor	CAR
Cytomegalovirus	*cmv*
Death-inducing Signaling Complex	DISC
Endoplasmic Reticulum	ER
Ethylenediaminetetraacetic Acid	EDTA
Eukaryotic Initiation Factor	eIF
Fatty Acid Synthase Ligand	FasL
Fas-associated Death Domain	FADD
Fas-receptor	FasR
Fetal Bovine Serum	FBS
Immunoglobulin	Ig
Inositol-requiring 1	IRE1
Interferon	IFN
Interleukin	IL
Mammalian Target of Rapamycin	mTOR
Melanoma Differentiation-associated 7	*mda-7*
Micro (10^{-6})	μ
Milli (10^{-3})	m
Minimum Essential Medium Alpha	MEMα
Mitogen-activated Protein Kinase	MAPK
Multiplicity of Infection	M.O.I.
Myeloid Cell Leukemia Sequence 1	MCL-1
Phosphate Buffered Saline	PBS
Plaque Forming Unit	pfu
Phosphoinositide 3-kinases	PI3K
Polyacrylamide Gel Electrophoresis	PAGE
Protein kinase-like Endoplasmic Reticulum Kinase	PERK
Quality Sufficient	QS

Renal Cell Carcinoma	RCC
Second Mitochondria-derived Activator of Caspases	SMAC
Sodium Dodecyl Sulfate	SDS
Surfactant-Free Cellulose Acetate	SFCA
Tetramethylethylenediamine	TEMED
Tris(hydroxymethyl)aminomethane	Tris
Tris buffered saline solution + Tween 20	TBST

ABSTRACT

Small Molecule Inhibitors of MAPK and PI3K Pathways Enhance MDA-7 Lethality in Renal Cell Carcinoma

By: Patrick John Eulitt

A thesis submitted in partial fulfillment of the requirements for the degree of Master of Science at Virginia Commonwealth University

Virginia Commonwealth University, 2010

Major Director: Dr. Paul Dent, Vice Chair of Research, Department of Neuro-Oncology

Renal cell carcinoma accounted for an estimated 57,760 new cases and estimated 12,980 deaths in the United States in 2009. Current treatment options for systemic renal cell carcinoma yield markedly low response percentages; however, recent cytokine therapy experiments have produced promising results. A novel adenovirus, Ad.5/3-*mda-7*, has been synthesized to efficiently infect renal cancer cells with the *mda-7* gene. This gene encodes for the cytokine MDA-7/IL-24 that has the ability to specifically target transformed cells. Assays performed with this adenovirus resulted in an increased percentage of cell death in renal cancer cells when compared to infection with Ad.5/3-*cmv* empty vector. Further assays that combined Ad.5/3-*mda-7* infection with treatments of small molecule inhibitors increased the percentages of cell death by upregulating JNK and p38 MAPK pathways, downregulating the ERK1/2 MAPK pathway, and downregulating the PI3K pathway. Western blots confirmed upregulation and downregulation of these pathways by probing for key proteins. Renal cancer cells responded best to infection with Ad.5/3-*mda-7* and treatment with PD184352, PX866,

and Rapamycin. This combinatorial treatment caused a greater percentage of cell death than the sum of the two individual treatments, suggesting a synergistic inhibition of cell growth pathways. These findings suggest that the combination of Ad.5/3-*mda-7* and specific small molecule inhibitors has developmental potential as a novel and more efficient treatment option for systemic renal cell carcinoma.

CHAPTER ONE:

INTRODUCTION

1.1 Background

Cancer is a major cause of death worldwide. In the United States alone, a total of 562,340 deaths from cancer were projected to occur in 2009. Cancer still accounts for more deaths than heart disease in persons younger than 85 years of age, despite recent reductions in mortality and improvement of survival (Ahmedin et al. 2009). Renal cell carcinoma (RCC) is the eighth most commonly diagnosed cancer in the United States, accounting for an estimated 57,760 new cases and estimated 12,980 deaths in 2009 (Cersosimo, 2009).

Treatment options for RCC have been relatively limited in the past; RCC has been shown to respond poorly to cytotoxic chemotherapy, and previous cytokine immunotherapy only produces moderate activity for the significant resulting toxicity (Saylor et al. 2009). In recent years, new therapies have emerged including melanoma differentiation-associated 7 (interleukin-24) and treatment with small molecule inhibitors (Yacoub et al. 2003, Kapoor et al. 2009).

To develop novel therapies to combat the growth of tumor cells in RCC, numerous signaling pathways are currently being investigated. The primary goal of these pathways is to increase apoptosis of cancer cells. Apoptosis, also known as programmed cell death, is the most common mechanism used by the human body to eliminate unneeded or

damaged cells without the undesired effects of inflammation or cell leakage (Bree et al. 2002). Cell necrosis, the passive mode of cell death, does share certain characteristics with apoptosis, but two processes are morphologically and biochemically distinct. Apoptosis is characterized by cell shrinkage, membrane blebbing without loss of integrity, and chromatin condensation with non-random DNA fragmentation (Ziegler et al. 2004). Cells undergoing necrosis, however, exhibit cell swelling, loss of membrane integrity, and random degradation of DNA (Ziegler et al. 2004).

Apoptosis is regulated by many different cytoplasmic proteins and transcription factors, but all pathways require the activation of effector caspases which destroy vital proteins necessary for cellular survival (Lavrik et al. 2005). The two main signaling pathways leading to apoptosis are the intrinsic and extrinsic pathways.

The intrinsic pathway, also referred to as the mitochondrial pathway, is activated primarily in response to internal signals such as DNA damage. This stimulates the tumor suppressor protein p53, which activates pro-apoptotic proteins that, in turn, activate caspase proteins in the mitochondria (Hengartner 2000). Under normal conditions, anti-apoptotic proteins, such as Bcl-2 and Bcl-XL, maintain the fidelity of the mitochondrial membrane by inhibiting the pro-apoptotic proteins, including BAX, BAK, and BAD (Hengartner 2000). Under stressed conditions, p53 activates the pro-apoptotic proteins causing mitochondrial membrane permeabilization and subsequent release of cytochrome c and SMAC/Diablo (Henry-Mowatt et al. 2004). Cytochrome c then binds to the apoptotic protease activating factor-1 (Apaf-1) and caspase-9 to form the aposome which

is able to activate the downstream caspases 3, 6, and 7 (Henry-Mowatt et al. 2004). For a visual representation of this pathway, see Figure 1 below.

The extrinsic pathway, as the name suggests, begins outside of the cell with the activation of pro-apoptotic receptors on the cell surface which are activated by specific molecules. One example of these receptor/ligand interactions is CD95L/FasL binding to CD95/Fas (Fulda et al. 2006). Other well characterized death receptors include TNF-related apoptosis-inducing ligand-receptor 1 (TRAIL-R1), TRAIL-R2, and TNF receptor 1 (Fulda et al. 2006). When the ligand binds to the appropriate receptor, there is induced receptor clustering which brings the adaptor protein Fas-associated death domain (FADD) to the activated receptor, which in turn recruits caspase-8 (Fulda et al. 2006). This aggregate cluster is better known as the death inducing signaling complex (DISC) (Kischkel et al. 1995). Pro-caspase molecules then migrate towards the DISC where they are processed and can activate effector caspases 3, 6, and 7 (Fulda et al. 2006). These caspases then proceed to destroy cellular proteins vital for survival, effectively killing the cell. This pathway can be visualized in Figure 2 below.

Mitogen Activated Protein Kinase (MAPK) pathways are also excellent targets for regulation of cell survival, particularly the ERK1/2, JNK1/2 and p38 modules (Boldt et al. 2002). In general, MAPK pathways work via three core kinases: a MAPKKK activates a MAPKK, which activates a MAPK. JNK and p38 are both the MAPK of their respective modules and after activation from cellular stress can signal the cell to undergo apoptosis. ERK1/2 is the MAPK of its module and signals for growth differentiation and

development. After receiving developmental cues from growth factors, ERK1/2 can promote cell differentiation (Boldt et al. 2002, Dent et al. 2009). The PI3K pathway functions to regulate cell growth in a similar manner to the ERK1/2 MAPK module, although it is morphologically distinct from the MAPK cascades (Dent et al. 2009). These 3 MAPK pathways, in addition to the PI3K pathway, are shown in Figure 3 below.

Another physiological response that can lead to cell death is the ER stress response, which is caused by an accumulation of misfolded or unfolded proteins accumulating in the ER. This aggregation of unfolded proteins is toxic to cells; therefore, these unfolded proteins trigger the unfolded protein response, which increase the folding capacity, inhibit protein translation and promote degradation of misfolded proteins (Hosoi et al. 2010). ER stress related signal transduction, which is shown in Figure 4, will lead to apoptosis via inhibition of anti-apoptotic proteins and activation of the JNK MAPK pathway (Hosoi et al. 2010). IRE1 is a transmembrane protein that signals in response to unfolded and misfolded proteins in the ER. When activated, IRE1 forms a complex with ASK1 which phosphorylates JNK, causing an induction of cell death (Rasheva et al. 2009). PERK is another ER-resident protein that signals in response to ER stress; however, it is distinct from IRE1 in its signaling cascade. PERK, when phosphorylated, will phosphorylate the α-subunit of eIF2, which promotes the translation of ATF4 (Hosoi et al. 2010). This transcription factor activates the CHOP promoter in the nucleus, causing an increase in production of the CHOP protein. By inhibiting anti-apoptosis proteins such as BCL-XL, BCL-2, and MCL-1, CHOP can sensitize cells to ER stress

induced apoptosis (Rasheva et al. 2009). Therefore, two discrete pathways can lead to cell death via ER stress.

Past therapeutic approaches for RCC, including chemotherapy and radiotherapy have yielded strikingly low response percentages, often as low as 2-6% (Bleumer et al. 2003). The low response can be partially accounted for by the resistance of renal cancer cells to the drugs being dispensed. Cytokine immunotherapy is currently being investigated to treat RCC with varied results (Herrmann et al. 2010). One particularly successful cytokine being investigated, melanoma differentiation-associated gene-7/interleukin-24 (MDA-7/IL-24), has been shown to inhibit the proliferation of renal carcinoma cells and promote cell death (Yacoub et al. 2003).

The gene *mda-7*was first identified in 1995 using differentiation induction subtraction hybridization (DISH), a novel technique that identifies differentially expressed genes in proliferating cancer cells and non-proliferating cancer cells (Fisher et al. 2003). Further experiments with this gene found little to no RNA products in differentiating cancer cells, elevated RNA expression in normal cells, and inducible expression in terminally differentiated cancer cells (Fisher et al. 2003). The unique properties of this cytokine identified in later experiments include its ability to discriminate between cancer cells and normal cells, inhibit tumor growth, induce apoptosis, and provide bystander antitumor activity (Fisher 2005).

Experiments suggesting bystander antitumor activity of MDA-7/IL-24 began as early as 2001, but no definitive *in vivo* evidence was published on this topic until 2005. Human breast carcinoma cells were inoculated into both flanks of nude mice, but only the left tumor was injected with Ad.*mda-7*. This injection resulted in tumor regression in the left side and a statistically significant regression in the right side tumor as well, confirming the "bystander" anti-tumor properties of the secreted MDA-7/IL-24 protein (Emdad et al. 2009).

Although *mda-7* was first identified in melanocytes, this gene was quickly tested on a wide range of human tumor cells with marked success. The most efficient method of infecting tumor cells with *mda-7* is to construct an adenovirus to efficiently insert the gene into cells (Fisher et al. 2003). Adenoviruses insert DNA into the host cell via coxsackievirus and adenovirus receptors (CAR). Therefore, the recombinant type 5 adenovirus to express *mda-7*/IL-24 (Ad.*mda-7*) was generated and proved to be an efficient method to insert *mda-7*/IL-24 into cancer cells (Fisher 2005). Unlike most cancer cells, RCC cells were found to be resistant to type 5 adenoviruses due to their low expression of CAR (Yacoub et al. 2003). A recent paper outlining the potential therapeutic benefits of MDA-7/IL-24 on RCC also noted the necessity of developing a modified adenovirus to infect kidney cancer cells at a location other than the CAR (Park et al. 2009). Fortunately, the development of a chimeric adenovirus, Ad.5/3-*mda-7*, has recently been developed to treat prostate cancer cells which also have a low expression of CAR. This new adenovirus targets the Ad.3 receptors in a CAR-independent manner to more efficiently transfer the DNA to prostate cancer cells and induce cell death (Dash et

al. 2010). It has been hypothesized that Ad.5/3-*mda-7* would also work to effectively infect kidney cancer cells, due to the Ad.3 receptor targeting instead of CAR receptor targeting.

Multiple signal pathways regulate MDA-7/IL-24-induced apoptosis, one of which includes inducing the ER-stress response and downstream MAPK enzymes (Fisher 2005). Other pathways affected by MDA-7/IL-24 include the extrinsic and intrinsic pathways mediating programmed cell death (Fisher 2005). More recent studies have determined the mechanism of MDA-7/IL-24-induced killing in renal carcinoma cells to be ceramide/CD95/PERK-dependent accompanied by strong activation of JNK1/2 and p38 MAPK pathways (Park et al. 2009). Although MDA-7/IL-24 has been shown to be successful in treating cancer cells, it has been suggested that combining MDA-7/IL-24 with small molecule inhibitors would provide the most profound therapeutic effects (Fisher 2005).

One such inhibitor, PD184352, was discovered in 1999 in an assay to identify small molecule inhibitors of the MAPK pathway (Sebolt-Leopold et al. 1999). This compound, shown below in Figure 5, was found to directly inhibit MEK1 which would decrease activation of the downstream kinase, ERK. In vivo treatment with PD184352 has been shown to result in complete suppression of MAPK phosphorylation in tumors, suggesting that it would be a great candidate for a combinatorial treatment with MDA-7/IL-24 (Sebolt-Leopold et al. 1999).

PI-103 is another small molecule inhibitor which was first synthesized in 2007 and has been found to have many beneficial effects in cancer therapy (Raynaud et al. 2007). The molecular structure of PI-103 is shown below in Figure 5. Unlike PD184352, PI-103 is a selective class I Phosphoinositide 3-kinase (PI3K) inhibitor which has been shown to inhibit the proliferation of cancer cells in vitro (Raynaud et al. 2007). PI-103 has also been shown to inhibit the mammalian target of rapamycin (mTOR), which is responsible for activating anti-apoptotic proteins (Chaisuparat et al. 2008). By inhibiting class I PI3K, PI-103 also significantly lowers the activation of AKT, which has been shown to halt the G_1 cell cycle progression and increase apoptosis (Erhardt et al. 1996, Gao et al 2004). Due to its activation of apoptosis via AKT and mTOR inhibition, PI-103 could potentially augment cellular apoptosis when treated with MDA-7/IL-24.

PX866, shown below in Figure 5, is a small molecule inhibitor which was first synthesized in 2004 along with 9 other similar drugs. Like PI-103, PX866 inhibits PI3K and downstream cellular AKT which halts growth and increases apoptosis in affected cells (Ihle et al. 2004). Additionally, PX866 has also been shown to have antitumor activity on colon cancer cells and has been hypothesized to have antitumor properties in other cancer cell lines (Ihle et al. 2004). PX866 was also tested in combination with other drugs and was found to act in a synergistic manner to kill tumors, which leads to the possibility of using PX866 in combination with MDA-7/IL-24.

Rapamycin is the last small molecule inhibitor that was tested in this project, and it can be seen below in Figure 5. Rapamycin is often referred to as Sirolimus, its United States

Adopted Name-assigned generic name, but for the purposes of this project, the name rapamycin will be used. Rapamycin was first isolated from a soil sample from Easter Island and was used as an antifungal agent prior to its use as an antitumor and immunosuppressive drug (Sehgal 2003). The mechanism underlying its antitumor properties begins with its association with a family of binding proteins termed FKBPs. Once rapamycin and FKBPs have associated, the complex can then bind directly to mTOR and block its function (Sehgal 2003). Inhibiting the function of mTOR causes downstream inhibition of AKT which leads to an arrested cell cycle and decreased cell growth. Like the other small molecule inhibitors, rapamycin has been tested in combination with other drugs, such as 5-flurouracil and cyclophosphamide, leading to the hypothesis that it would work well with MDA-7/IL-24.

A recent phase I clinical trial with Ad.*mda-7* aimed to take knowledge of *mda-7* from the bench into the clinic, and was considered a resounding success. The translational work was designed to evaluate the efficacy of intratumoral injection of Ad.*mda-7* in patients with advanced carcinoma (Emdad et al. 2009). All twenty-eight patients that enrolled in the study tolerated the adenovirus injection, all tumors injected demonstrated MDA-7/IL-24 protein expression and apoptosis induction, and nearly half of the patients showed a marked decrease in tumor size at the conclusion of the study (Emdad et al. 2009). The most clinically significant responses were seen in patients that received repeat injections of Ad.*mda-7*, but combining Ad.*mda-7* with other inhibitory agents has been suggested to further enhance antitumor activity of the virus (Emdad et al. 2009).

The case for combinatorial therapies for cancer patients stems from the inability to translate *in vitro* tumor suppression of single inhibitory agents into the clinic. When single kinase inhibitory agents were tested *in vivo*, the treatments were no longer cytotoxic; instead the agents seemed to be cytostatic (Dent et al. 2009). The concept of pathway crosstalk has recently been suggested as an explanation to this reduction in response; it is possible that when one pathway is inhibited, another pathway that elicits a similar response may be upregulated (Junttila et al. 2008). Only a small minority of cancerous tumors have a single mutation causing the uncontrolled growth. Therefore, the current theory calls for targeting multiple signal pathways to provide a more profound response in tumor cells (Dent et al. 2009).

1.2 Objectives

The first objective of this project was to determine if the newly synthesized adenovirus Ad.5/3-*mda-7* would efficiently infect and increase the percentage of cell death in renal cancer cells, represented by the A498 cell line. A secondary objective was to determine the most efficient treatment of small molecule inhibitors to enhance the toxicity of Ad.5/3-*mda-7* in renal cancer cells. The final objective was to confirm the mechanisms by which the adenovirus and small molecule inhibitors increase cell death.

Figure 1

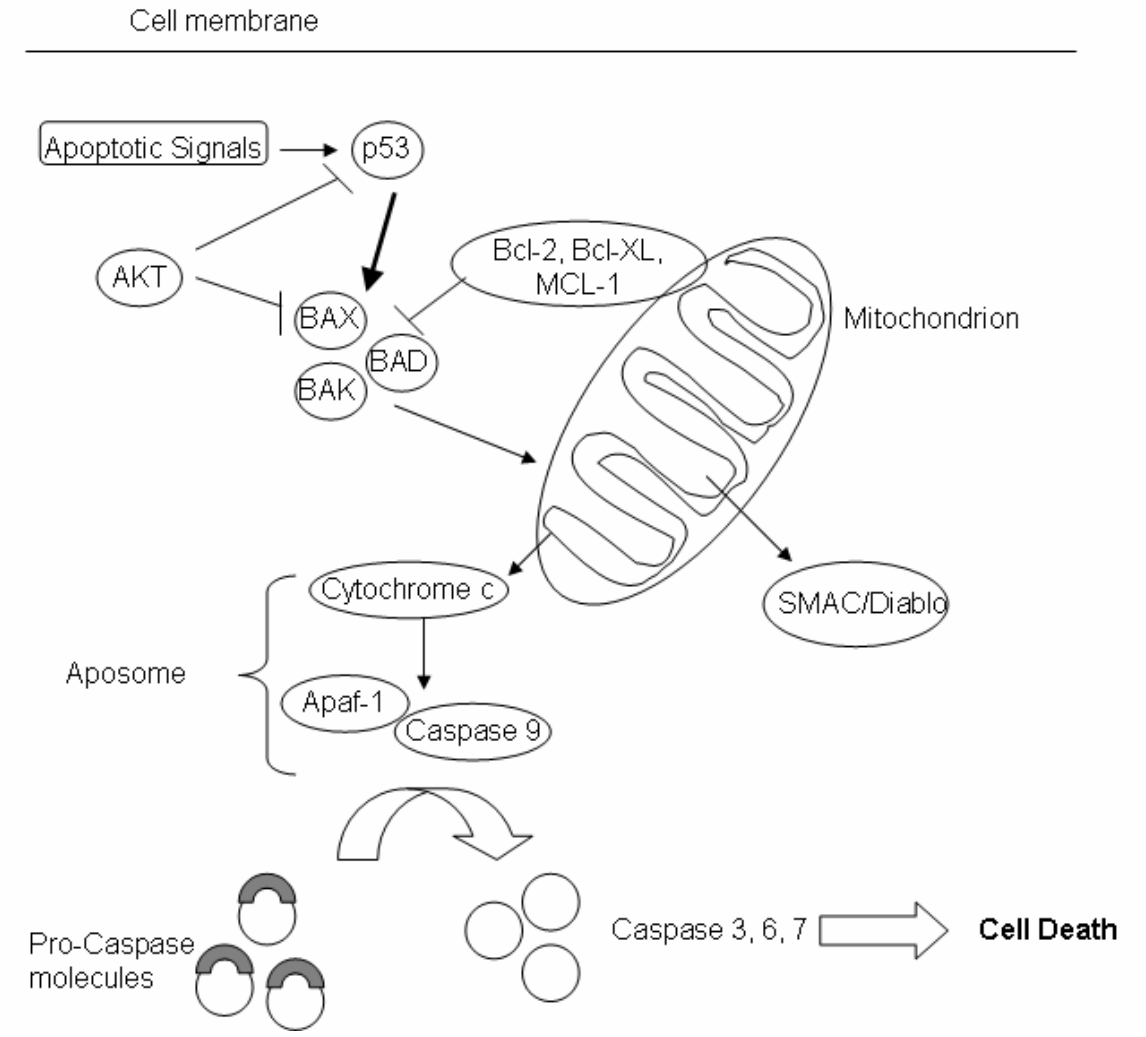

Figure 1: Intrinsic pathway of apoptosis activation

(Adapted from Hengartner 2000 and Henry-Mowatt et al. 2004)

Figure 2

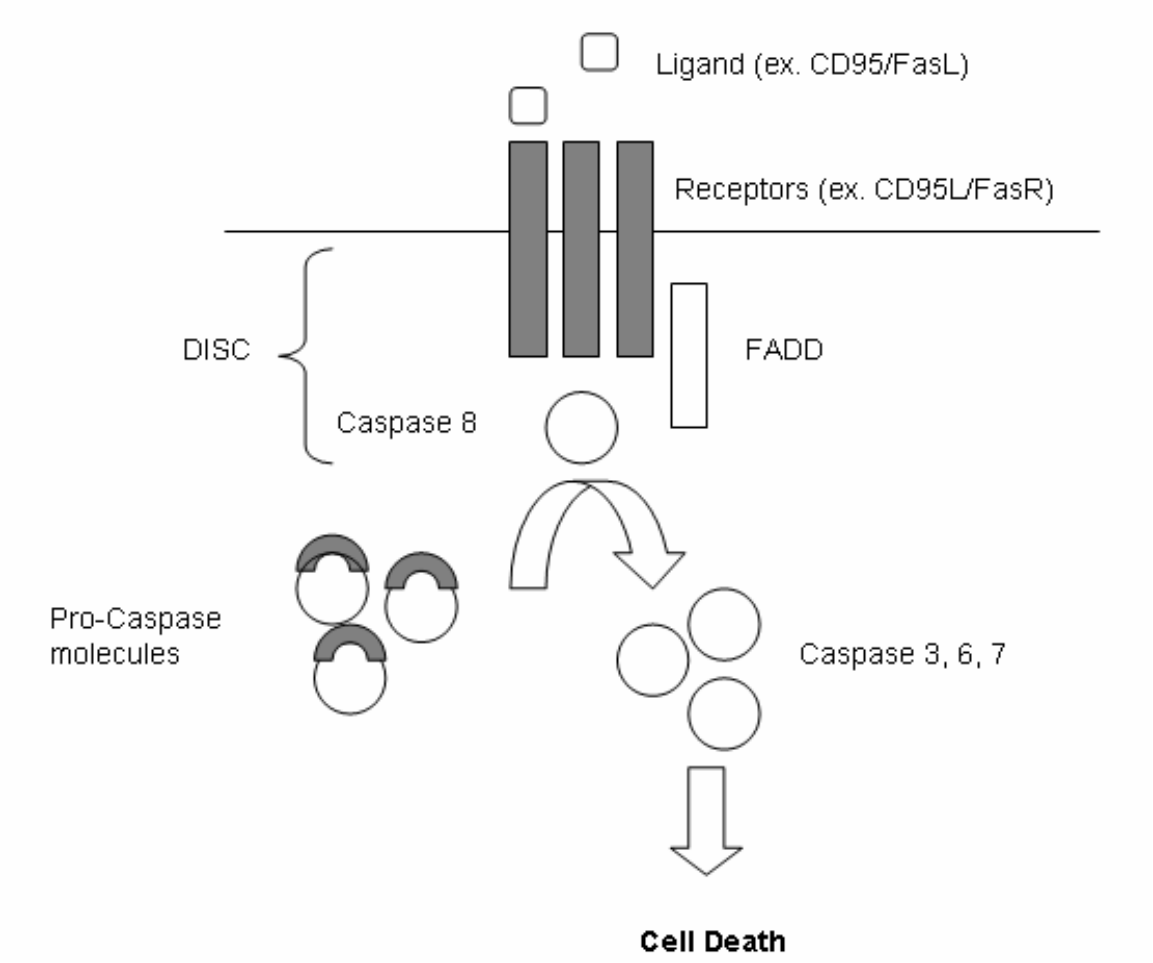

Figure 2: Extrinsic pathway of apoptosis activation

(Adapted from Fulda et al. 2006)

Figure 3

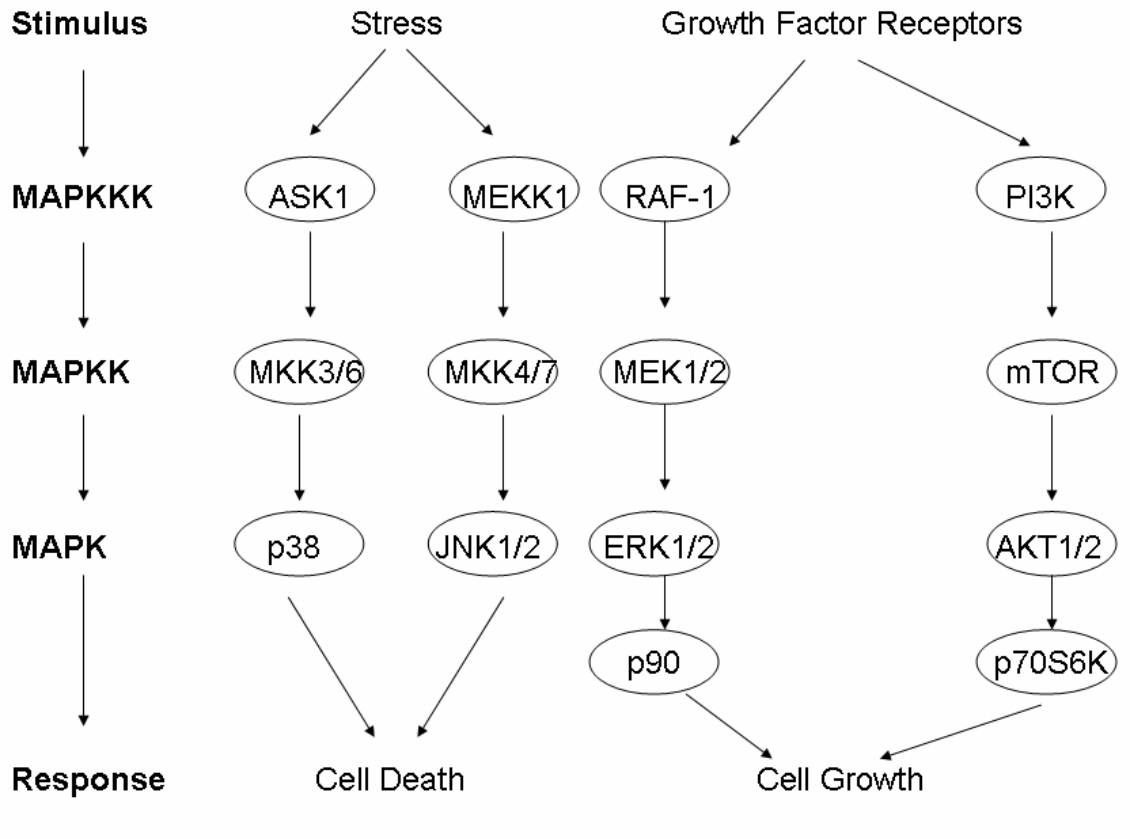

Figure 3: Summary of signal transduction pathways targeted

via small molecule inhibitors and MDA-7/IL-24

(Simplified version of Dent et al. 2009)

Figure 4

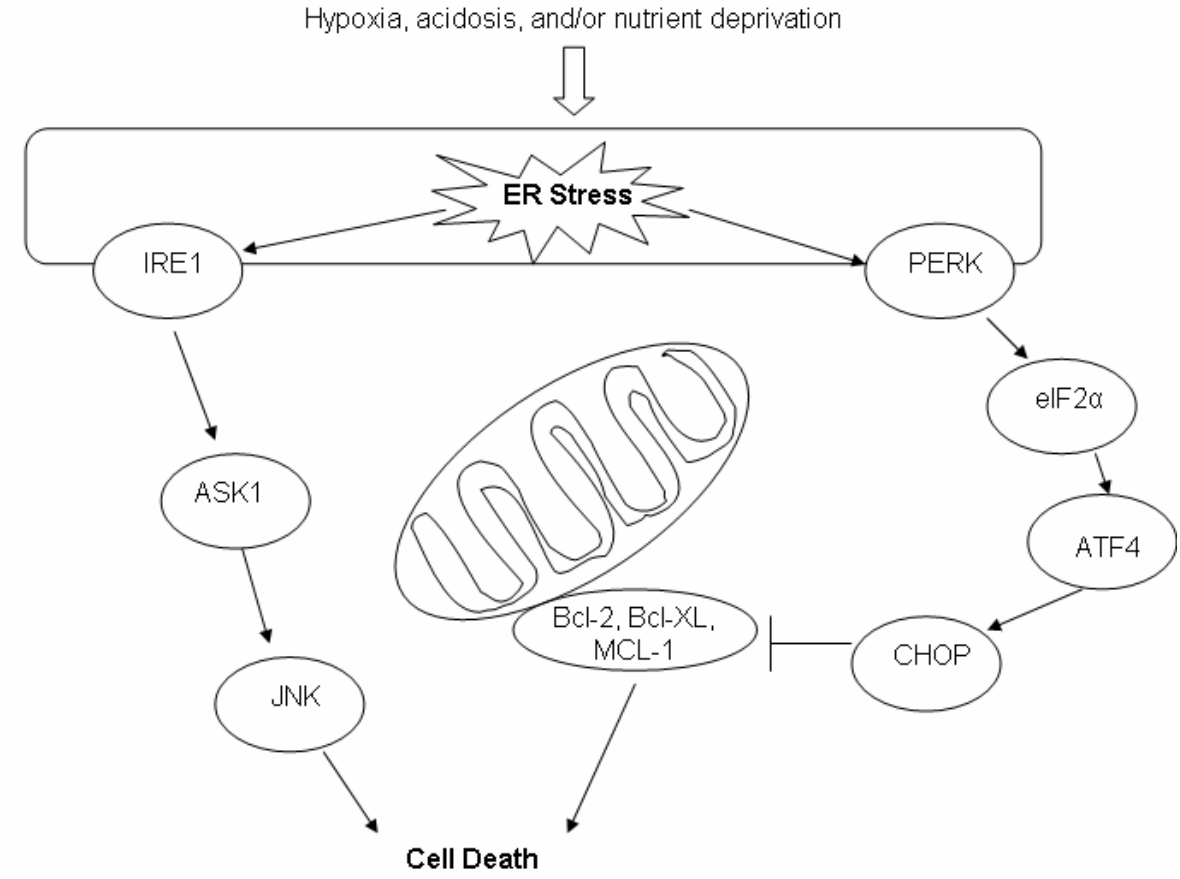

Figure 4: ER stress related signal transduction pathways leading to apoptosis

(Adapted from Rasheva et al. 2009 and Hosoi et al. 2010)

Figure 5

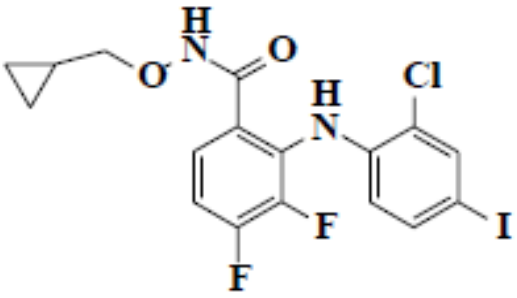

PD184352
(Sebolt-Leopold et al. 1999)

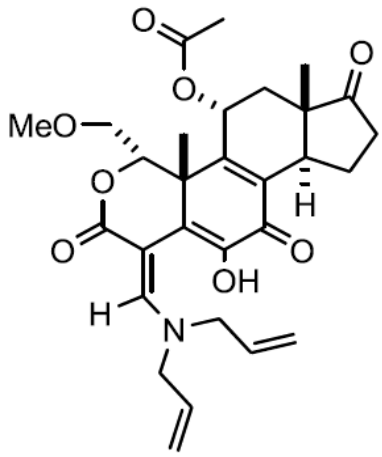

PX866
(Ihle et al. 2004)

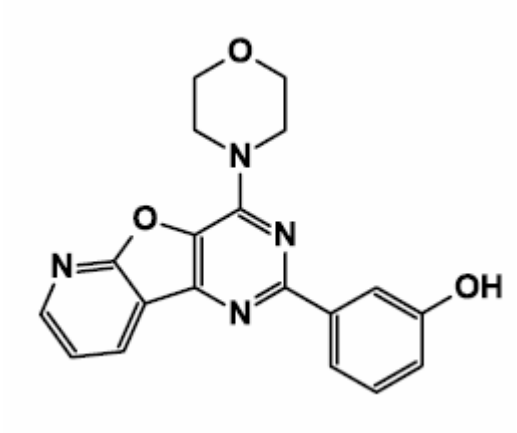

PI-103
(Raynaud et al. 2007)

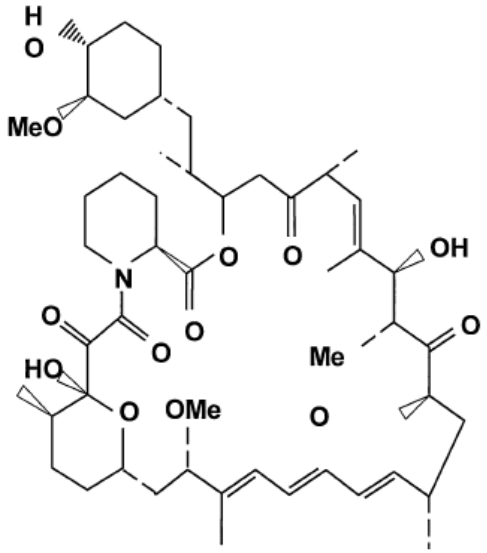

Rapamycin
(Sehgal 2003)

Figure 5: Chemical structures of small molecule inhibitors of MAPK pathway (PD184352) and PI3K pathway (PI-103, PX866, and Rapamycin)

CHAPTER TWO:

MATERIALS AND METHODS

2.1 Materials

Minimum Essential Medium Alpha (MEMα), penicillin-streptomycin, 0.25% trypsin-EDTA, and secondary antibody anti-mouse IgG were purchased from Invitrogen Life Technologies, Inc. (Carlsbad, CA). The composition of MEMα is shown below in Table 1. Anti-phospho-p38 MAP Kinase (43 kDa, 1:000, rabbit polyclonal), anti-phospho-SAPK/JNK (46, 54 kDa, 1:000, rabbit polyclonal), anti-MCL-1 (40 kDa, 1:1000, rabbit polyclonal), anti-mTOR (289 kDa, 1:1000, rabbit polyclonal) and anti-phospho-mTOR (289 kDa, 1:1000, rabbit polyclonal) were obtained from Cell Signaling (Boston, MA). Anti-BAX (23 kDa, 1:000, mouse monoclonal), anti-phospho- Akt1/2 (60 kDa, 1:1000, rabbit polyclonal), anti-phospho-eIF2 α (38 kDa, 1:1000, rabbit polyclonal), anti-eIF2α (36 kDa, 1:1000, rabbit polyclonal), anti-phospho-ERK (42, 44 kDa, 1:1000, mouse monoclonal), anti-GAPDH (37 kDa, 1:000, mouse monoclonal), and anti-phosho-PERK (125 kDa, 1:1000, rabbit polyclonal) were obtained from Santa Cruz Biotechnology (Santa Cruz, CA). Secondary antibody anti-rabbit IgG was purchased from Rockland Immunochemicals (Gilbertsville, PA).

Table 1

COMPONENTS	Molecular Weight	Concentration (mg/L)	mM
Amino Acids			
Glycine	75	50	0.667
L-Alanine	89	25	0.281
L-Alanyl-L-Glutamine	203	406	2
L-Arginine	211	105	0.498
L-Asparagine-H2O	132	50	0.379
L-Aspartic acid	133	30	0.226
L-Cysteine hydrochloride	121	100	0.826
L-Cystine	313	31	0.099
L-Glutamic Acid	147	75	0.51
L-Histidine	155	31	0.2
L-Isoleucine	131	52.4	0.4
L-Leucine	131	52.4	0.4
L-Lysine	146	58	0.397
L-Methionine	149	15	0.101
L-Phenylalanine	165	32	0.194
L-Proline	115	40	0.348
L-Serine	105	25	0.238
L-Threonine	119	48	0.403
L-Tryptophan	204	10	0.049
L-Tyrosine	181	36	0.199
L-Valine	117	46	0.393
Vitamins			
Ascorbic Acid	176	50	0.284
Biotin	244	0.1	0.00041
Choline chloride	140	1	0.00714
D-Calcium pantothenate	477	1	0.0021
Folic Acid	441	1	0.00227
Niacinamide	122	1	0.0082
Pyridoxal hydrochloride	204	1	0.0049
Riboflavin	376	0.1	0.000266
Thiamine hydrochloride	337	1	0.00297
Vitamin B12	1355	1.36	0.001
i-Inositol	180	2	0.0111
Inorganic Salts			
Calcium Chloride (CaCl2-2H2O)	147	264	1.8
Magnesium Sulfate (MgSO4-7H2O)	246	200	0.813
Potassium Chloride (KCl)	75	400	5.33
Sodium Bicarbonate (NaHCO3)	84	2200	26.19
Sodium Chloride (NaCl)	58	6800	117.24
Sodium Phosphate monobasic (NaH2PO4-2H2O)	156	158	1.01
Other Components			
D-Glucose (Dextrose)	180	1000	5.56
Lipoic Acid	206	0.2	0.000971
Phenol Red	376.4	10	0.0266
Sodium Pyruvate	110	110	1

Table 1: Composition of MEMα used for cell culture. Data taken from Invitrogen website:

http://www.invitrogen.com/site/us/en/home/support/Product-Technical-Resources/media_formulation.109.html

2.2 Cell Culture

The human renal cell carcinoma cell line, A498, was purchased from American Type Culture Collection (Rockville, MD). This cell line was cultured in MEMα (Invitrogen) supplemented with 10% (v/v) FBS (American Type Culture Collection, Manassas, VA) and 2% penicillin/streptomycin. Media was filtered using a 500 mL SFCA filter unit (Fisher Scientific: Kalamazoo, MI) to remove any impurities. Cells were incubated in a humidified atmosphere of 5% (v/v) CO_2 at 37°C. Cells were plated at a minimum density of 2×10^5 per cm^2.

2.3 Recombinant Adenovirus Vectors: *in vitro* infection

The Ad.5/3-*mda*-7 and Ad.5/3-*cmv* empty vector control adenoviral vectors used for the following experiments were generously provided by Dr. Paul Fisher (Department of Human and Molecular Genetics, Virginia Commonwealth University). The stock concentrations for the adenoviruses used were as follows:

Ad.5/3-*mda-7* = 4.5×10^{12} pfu/mL

Ad.5/3-*cmv* empty vector = 2.15×10^{12} pfu/mL

After cells were allowed to grow for 24 hours, the cells were then infected with either Ad.5/3-*mda*-7 or Ad.5/3-*cmv* empty vector to obtain a multiplicity of infection (M.O.I.) of 50.

M.O.I. = [(desired m.o.i)*(# of cells)]/(titer of virus)

Prior to infection, the adenoviruses were diluted in serum-free MEMα. The complete media was aspirated from the plates, and the diluted Ad.5/3-*mda*-7 or Ad.5/3-*cmv* empty vector was added. The plates were then placed on a rocker for 4 hours at the same

atmosphere in which cells are incubated: 5% (v/v) CO_2 at 37°C. After the media with the virus was aspirated from the plates 4 hours after infection, fresh 10% (v/v) FBS MEMα was added and the plates were returned to the incubator.

2.4 Treatment with PD184352, PI-103, PX866, and Rapamycin

24 hours after infection with Ad.5/3-*mda*-7 or Ad.5/3-*cmv* empty vector, cells were given drug treatments to further increase cell death. The four drugs used were: PD184352, PI-103, PX866 and Rapamycin. Some experiments called for combinations of drugs; these combinations were: PD184352+PI-103, PD184352+PX866, PD184352+Rapamycin, and PD184352+PX866+Rapamycin. In order to treat the cells at the recommended dosages, the drugs first needed to be diluted in serum-free MEMα. Once the drugs were diluted into 2 mL dolphin Eppendorf tubes, the tubes were placed on a vortex for 2 intervals of 10 seconds. Drugs were added to the plates in the appropriate concentrations with the pipette tips replaced after each dish. Eppendorf tubes were placed on a vortex after treatment of 3 dishes to ensure consistency in drug treatments. Drug information can be found below in Table 2.

Table 2

Drug	Original Stock Conc.	Dilution	Final Conc.
PD184325	**50mM**	**1:25000**	**2μM**
PI-103	**10mM**	**1:20000**	**0.5μM**
PX866	**1mM**	**1:4000**	**0.25μM**
Rapamycin	**10mM**	**1:10000**	**1μM**

Table 2: Dilution information for drugs used in the following experiments

2.5 Cell Lysis

Cells were cultured in 60 mm dishes for 24 hours, after which they were infected with either Ad.5/3-*mda-7* or Ad.5/3-*cmv* empty vector. 24 hours after infection, the cells were treated with the specified drug or drug combination. After incubation for six hours, the media was aspirated from the dishes and the dishes were immediately placed on a bed of ice. The cells were lysed in 200μL of 2x SDS blue sample buffer. This buffer solution contained 125 mM Tris-Cl, 20% (v/v) glycerol, 10% (v/v) β-mercaptoethanol, 4% (v/v) sodium dodecyl sulfate, and 0.04% (v/v) bromophenol blue at a pH of 6.8. The dishes were scraped with disposable cell lifters (Fisher Scientific) and the lysate was collected and placed into 2 mL dolphin Eppendorf tubes. These samples were boiled at 100°C for 10 minutes and immediately frozen at -30°C until ready to be used.

2.6 Polyacrylamide Gel Electrophoresis and Western Blot Analysis

To prepare a gel for gel electrophoresis, the following steps were taken. The glass plates were washed, rinsed with 70% (v/v) ethanol, and allowed to dry. Spacers were placed between the glass plates and single screw clamps were aligned to secure the plates and spacers in place. Once the bottom of the plates and spacers were aligned with the bottom of the screw clamps and Parafilm was placed in the BioRad casting stand, the contraption was secured and tightened into the stand. The resolving gel was prepared in accordance to the values in Table 3 in the following order: milli-Q water, 1.5 M Tris (pH 8.8), 40% acrylamide (Biorad), 10% (w/v) ammonium persulphate, and TEMED (Fisher Scientific, Suwannee, GA). Once the resolving gel was poured between the glass plates, 1 mL of saturated isobutanol was added to each gel. The concentration of acrylamide used varied

inversely with the molecular weight of the protein under investigation; if a high molecular weight protein was being analyzed, a low concentration of acrylamide was used to facilitate migration down the gel.

One hour following the addition of the resolving gel, the saturated isobutanol was removed from the gel, which was then gently cleaned with distilled water and carefully dried with Whatman 3M paper. The combs (either 15 well or 20 well) were then placed between the glass plates and the stacking gel was prepared in accordance to the values listed in Table 3 and poured over the resolving gel. Any air bubbles that formed around the wells were removed by shaking the comb before the stacking gel started to solidify.

One hour after the addition of the stacking gel, the combs were removed and the gel apparatus was assembled. To do this, the gels were removed from the casting stand and locked into place on the Protean 2 Gel Holder (Bio-Rad). 1X SDS Running buffer was prepared (6.00g Tris-base, 28.80g glycine, 10mL 20% SDS, QS to 2L deionized water) and poured between the two sets of glass plates. The Gel Holder was allowed to sit for five minutes to inspect for leaks. If the running buffer was leaking from the bottom of the gel, the screw clamps were tightened and the glass plates were inspected for cracks. Once the apparatus was determined to be leak free, it was placed in the gel case and the remaining running buffer was added until the case was about one-third full.

The gel was then loaded with 75µL lysate and 25µL Dual Color Precision Plus Protein Standards (Bio-Rad) into the appropriate wells. The gel apparatus was covered and

connected to a 200V power supply (Bio-Rad) and set to 475mA for two gels for about 5 hours, or until the bromophenol blue dye front reached the bottom of the resolving gel.

The next step in this process is transferring the protein from the gel to a 0.22μm nitrocellulose membrane (GE Water & Process Technologies). In order to do so, it was first necessary to prepare the transfer solution, consisting of 9.09g Tris-base, 43.2g glycine, 15mL 20% SDS, 600mL methanol, and 2.1 L of deionized water. This transfer solution was then degassed and allowed to cool at 4°C for two hours.

Transfer solution was poured into 2 glass pans where the transfer cassette would be assembled. A third glass pan was filled with deionized water. A transfer cassette, 4 pieces of Whatman 3M paper, 2 foam pads, and a sheet of nitrocellulose were gathered for each gel transfer. The 0.22μm nitrocellulose membrane was placed in the water bath to check for uneven saturation. If the membrane was evenly saturated, the nitrocellulose was transferred to the glass pan with the transfer buffer. The items gathered were placed in the transfer cassette in the following order: one foam pad, two pieces of Whatman 3M paper, acrylamide gel, nitrocellulose membrane, two pieces of Whatman 3M paper, one foam pad. Care was taken to ensure that there were no air pockets between the layers of materials, which would produce spots on the nitrocellulose membrane during development. The locked transfer cassette was then placed in the transfer box so the current would run through the gel onto the nitrocellulose, and the transfer box was filled with the remaining transfer solution. After connection to a 200V power source, the transfer box was set at 475mA for 5 hours.

Once 5 hours had passed, the transfer cassette was opened and the nitrocellulose was checked for the protein standards. If the protein standards had transferred to the nitrocellulose membrane, it was assumed that the protein samples had also transferred to the membrane. This nitrocellulose membrane was removed from the cassette, placed in a plastic container, and rinsed for 5 minutes with Tris Buffered Saline buffer (TBST): 24.22g Tris-base, 18g NaCl, 1mL Tween 20 (Bio-Rad), QS to 1L deionized water. After rinsing in TBST, the membrane was placed in a blocking buffer: 25g Blotting Grade Blocker Non-Fat Dry Milk (Bio-Rad), QS to 500mL TBST. The membrane was kept in blocking buffer on a shaker for one hour at 4°C. The primary antibody for the desired protein was then added to the blocking buffer in dilutions appropriate for the antibody (usually 1:1000) and was sealed with Saran wrap. The covered nitrocellulose was kept on a shaker overnight at 4°C.

The following day, the nitrocellulose was washed with TBST 3 times for 10 minutes to remove any non-specific primary antibody bonding. Blocking buffer was then added to the nitrocellulose again, along with diluted secondary antibody to the specific mammal used for the primary antibody. The nitrocellulose was then covered in Saran wrap and tin foil to prevent photobleaching of the secondary antibody, and kept at 4°C for one hour. After one hour, the nitrocellulose was washed 3 times for 10 minutes in TBST to remove any non-specific secondary antibody bonding and was read on the Odyssey Infrared Imager (Li-Cor) using Odyssey 2.1. Images were then scanned and exported into Adobe Photoshop.

Table 3

Solutions required for resolving gel for SDS-PAGE

Resolving Gel		One side	Two sides
	Components	50 mL	100 mL
10%	40% acrylamide	12.5	25.5
	1.5 M Tris (pH 8.8)	12.5	25
	10% AP	0.5	1
	TEMED	0.02	0.04
	H_2O	24.5	49
12%	40% acrylamide	15	30
	1.5 M Tris (pH 8.8)	12.5	25
	10% AP	0.5	1
	TEMED	0.02	0.04
	H_2O	22	44
14%	40% acrylamide	17.5	35
	1.5 M Tris (pH 8.8)	12.5	25
	10% AP	0.5	1
	TEMED	0.02	0.04
	H_2O	19.5	39

Solutions required for resolving gel for SDS-PAGE

Stacking Gel		One side	Two sides
	Components	10 mL	20 mL
5%	40% acrylamide	1.25	2.5
	0.5 M Tris (pH 6.8)	2.5	5
	10% AP	0.1	0.2
	TEMED	0.01	0.02
	H_2O	6.2	12.4

Table 3: Solutions required for the stacking and resolving gel for SDS-PAGE

Only 10%, 12%, and 14% gels were used for this paper. All volumes are in mL.

H_2O = milli-Q water, 10% AP= 10% (w/v) ammonium persulphate, TEMED (Fischer Scientific, Suwannee, GA)

2.7 Assessing Cell Death: Trypan Blue Exclusion Assay

One method for evaluating the number of viable cells present in a cell suspension is to use a trypan blue exclusion assay. Observed under light microscopy, viable cells with an intact membrane will exclude the trypan blue dye, whereas dead cells with a compromised membrane will include the dye. To perform this assay, cells were plated in 12-well plates with about 2 x 10^4 cells per well. After 24 hours, the cells were infected as described above, and 24 hours after infection, cells were treated as described above. At the specified time after treatment, the media was removed from each well and placed into a labeled 15mL tube. 185µL of trypsin was added to each well and the plates were incubated for 5 minutes. 500µL of PBS was then added to each well and the solution was mixed to ensure all the cells were in solution. The cells and remaining solution were added to the appropriate 15mL tubes and these tubes were centrifuged at 1400 rpm for 4 minutes. The media was then aspirated and 75µL of trypan solution was added to each tube (1mL Trypan Blue (Sigma Aldrich), 9mL PBS). The solution was mixed manually using a pipette for 2 minutes and loaded onto a hemocytometer. Cells were counted on all four fields of the hemocytometer and the percentage of cells including trypan blue was determined for each tube.

2.8 Statistical Analyses

The effects of the drug treatments were analyzed using one-way ANOVA and Student's t-test as a test for significance. Differences with a p-value less than 0.05 were considered statistically significant. Standard errors will be shown on the figures that follow.

CHAPTER THREE:

RESULTS

3.1 Infection with Ad.5/3-*mda-7* causes greater cell death than infection with Ad.5/3-*cmv* empty vector

Cells that were infected with Ad.5/3-*mda-7* had a higher percentage of cell death than cells that were infected with Ad.5/3-*cmv* empty vector, as assessed by trypan blue exclusion assay. This proved that Ad.5/3-*mda-7* was effective in infecting A498 renal cancer cell. These results can be seen by comparing similar treatments between Ad.5/3-*mda-7* and Ad.5/3-*cmv* empty vector infections in Figure 6 and 7 below. This supports past publications outlining the apoptosis inducing properties of MDA-7/IL-24 (Fisher et al. 2003, Fisher 2005).

3.2 Treatment with small molecule inhibitors enhances Ad.5/3-*mda-7* toxicity in RCC cells

When combined with Ad.5/3-*mda-7*, small molecule inhibitors increase the percentage of cell death in A498 cells above the vehicle. In Figures 6 and 7, nearly every treatment caused an increase in cell death, when compared to the vehicle. Combinatorial treatment methods have not previously been attempted in A498 cells with Ad.5/3-*mda-7* and these small molecule inhibitors, but the data suggest that a clinical trial may be warranted.

3.3 PD184352+PX866+Rapamycin provides greatest percentage of cell death, and treatment works synergistically with Ad.5/3-*mda-7*

Of all the combinatorial treatments assessed in this project, the most effective treatment was PD184352+PX866+Rapamycin. As seen in Figure 8, this treatment, combined with Ad.5/3-*mda-7* produced the lowest ratio of cell survival when compared to combination with Ad.5/3-*cmv* empty vector. Figure 9 offers a clearer depiction of the synergistic increased cell death caused by this treatment and Ad.5/3-*mda-7* infection. The empty vector adenovirus and the treatment caused about 20% cell death, and the *mda-7* adenovirus caused about 18% cell death. However, when Ad.5/3-*mda-7* was combined with the treatment, there was greater than 50% cell death, suggesting a synergistic interaction between the virus and small molecule inhibitor combination.

3.4 Western Blotting confirms ER stress induction, upregulation of JNK and p38 MAPK signaling, and downregulation of ERK MAPK signaling by Ad.5/3-*mda-7*

In a series of western blots, the Ad.5/3-*mda-7* infection was confirmed to cause ER stress induction. Figure 10 shows upregulation of P-PERK, P-eIF2α, and pro-apoptotic protein BAX in samples infected by Ad.5/3-*mda-7* as compared to samples infected by Ad.5/3-*cmv* empty vector. When ER stress is induced, CHOP is synthesized downstream to inhibit protective anti-apoptotic proteins in the mitochondria, such as MCL-1, which is drastically downregulated by Ad.5/3-*mda-7* in Figure 10 below. All proteins measured in Figure 10 can be seen Figure 4, the ER stress related signal transduction pathway leading to apoptosis.

Ad.5/3-*mda-7* also caused an upregulation of P-JNK and P-p38, both MAPK pathway proteins leading to apoptosis. Figure 11 below shows the western blots that confirmed these upregulations, and Figure 3 shows the relationship of JNK and p-38 in the MAPK cascade.

One pathway downregulated by Ad.5/3-*mda-7* was the ERK MAPK pathway that results in cellular growth. As seen in Figure 12, P-ERK1/2 expression is downregulated in samples infected with Ad.5/3-*mda-7* when compared to samples infected with Ad.5/3-*cmv* empty vector. Figure 3 shows the relationship of ERK 1/2 in the MAPK cascade. GAPDH was used as a loading control in Figures 10 and 11.

3.5 Western Blotting confirms inhibition of PI3K pathway by small molecule inhibitors

Additional western blotting was performed to confirm the action of PI3K pathway inhibitors, including probing for P-mTOR, mTOR, and P-AKT. Because Rapamycin inhibits mTOR, it was hypothesized that there would be a downregulation of P-mTOR, mTOR, and the downstream AKT, when compared to the vehicle. PX866 is a PI3K inhibitor which would downregulate downstream P-mTOR, mTOR, and P-AKT, when compared to the vehicle. All of these results can be seen in Figure 12 below. GAPDH was used as a loading control in Figure 12.

Figure 6

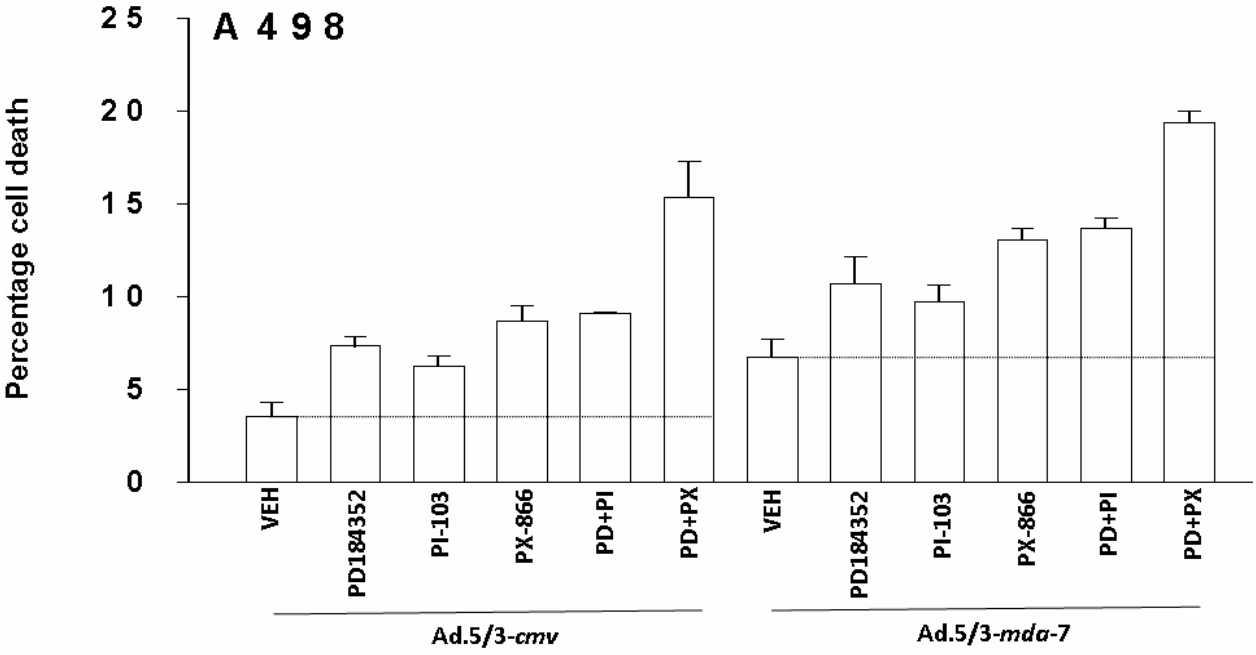

Figure 6: Infection with Ad.5/3-*mda-7* causes greater cell death in A498 cells than infection with Ad.5/3-*cmv* as evaluated by a trypan blue exclusion assay. Assay data are means of 3 wells (one column of 12 well plate per condition +/- SE) from representative experiment using different small molecule inhibitors and combinations of small molecule inhibitors (n=3). PD=PD184352, PI=PI-103, PX=PX866

Figure 7

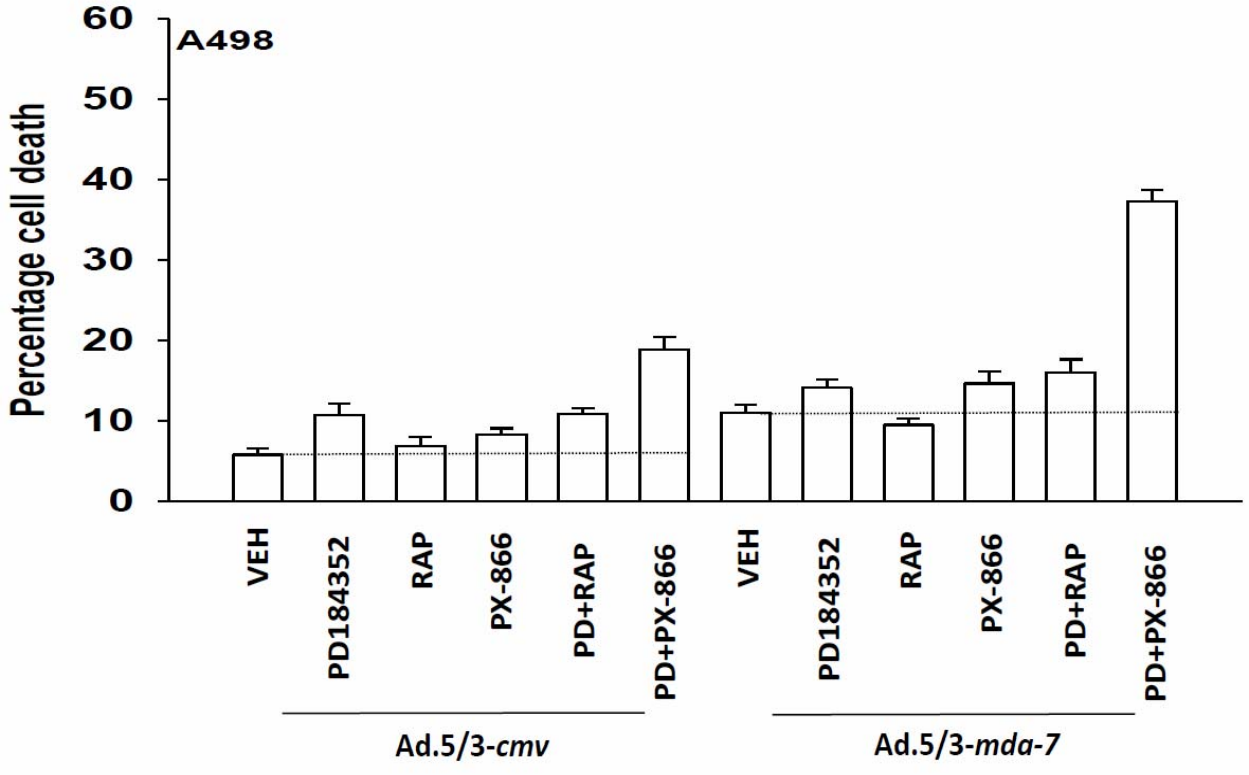

Figure 7: Infection with Ad.5/3-*mda-7* causes greater cell death in A498 cells than infection with Ad.5/3-*cmv* as evaluated by a trypan blue exclusion assay. Rapamycin was used in this assay instead of PI-103. Assay data are means of 3 wells (one column of 12 well plate per condition +/- SE) from representative experiment using different small molecule inhibitors and combinations of small molecule inhibitors (n=3).

PD=PD184352, RAP=Rapamycin

Figure 8

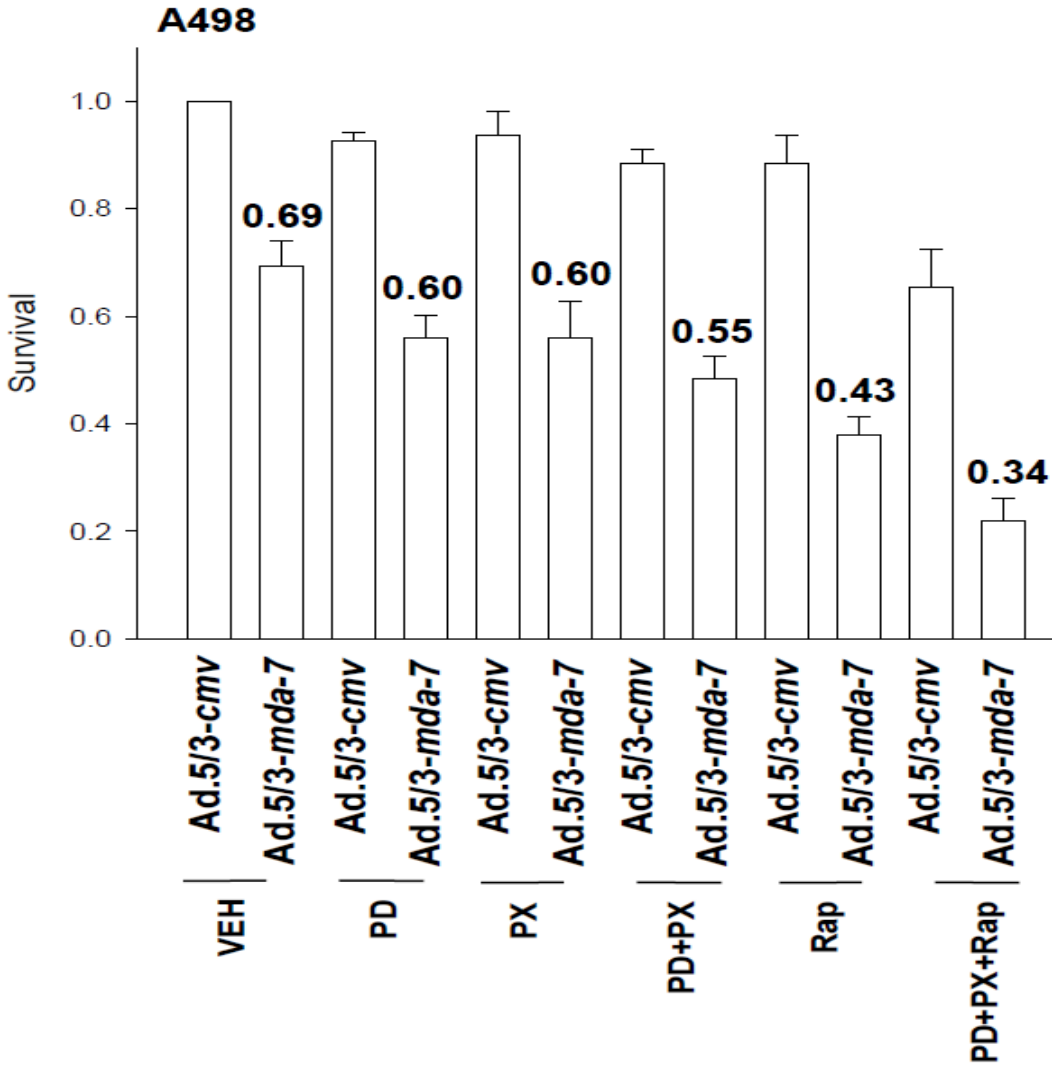

Figure 8: Ratio of cell survival (Ad.5/3-*mda-7* infection + treatment: Ad.5/3-*cmv* infection + treatment) smallest with PD184352+PX866+Rapamycin. Data were generated from trypan exclusion assays, and normalized Ad.5/3-*cmv* + VEH to 1.0 survival. Assay data are means of 3 wells (one column of 12 well plate per condition +/- SE) from representative experiment using different small molecule inhibitors and combinations of small molecule inhibitors (n=3). PD=PD184352, PX=PX866, RAP=Rapamycin

Figure 9

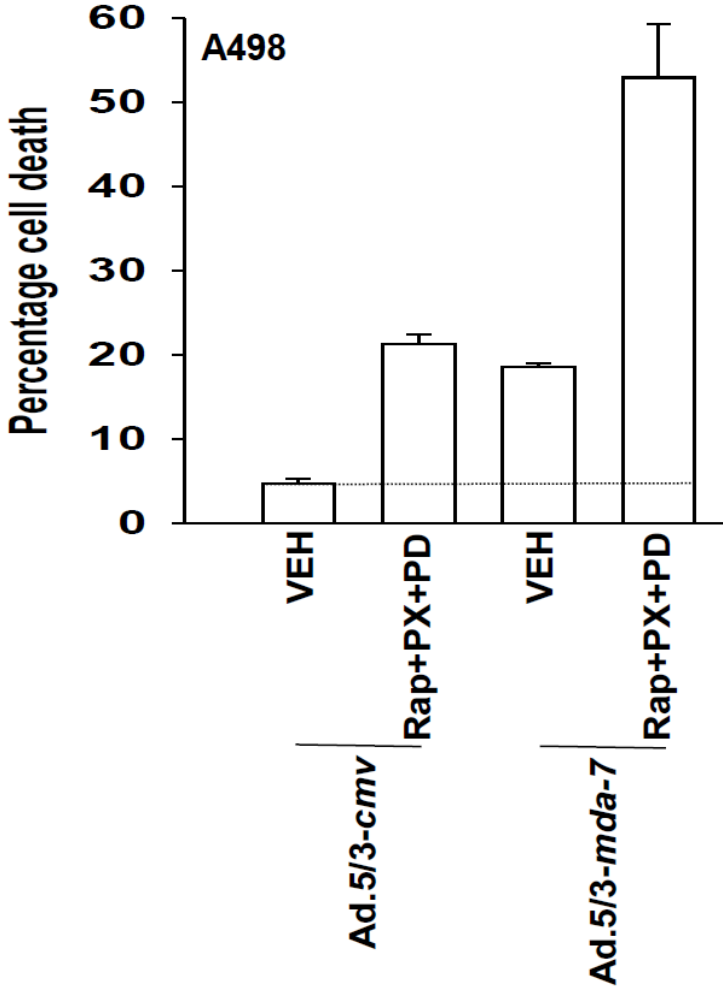

Figure 9: Infection with Ad.5/3-*mda-7*, combined with treatment of PD184352+PX866+Rapamycin, was the most effective therapy for A498 RCC cells. Assay data are means of 3 wells (one column of 12 well plate per condition +/- SE) from representative experiment using different small molecule inhibitors and combinations of small molecule inhibitors (n=3). PD=PD184352, PX=PX866, Rap=Rapamycin

Figure 10

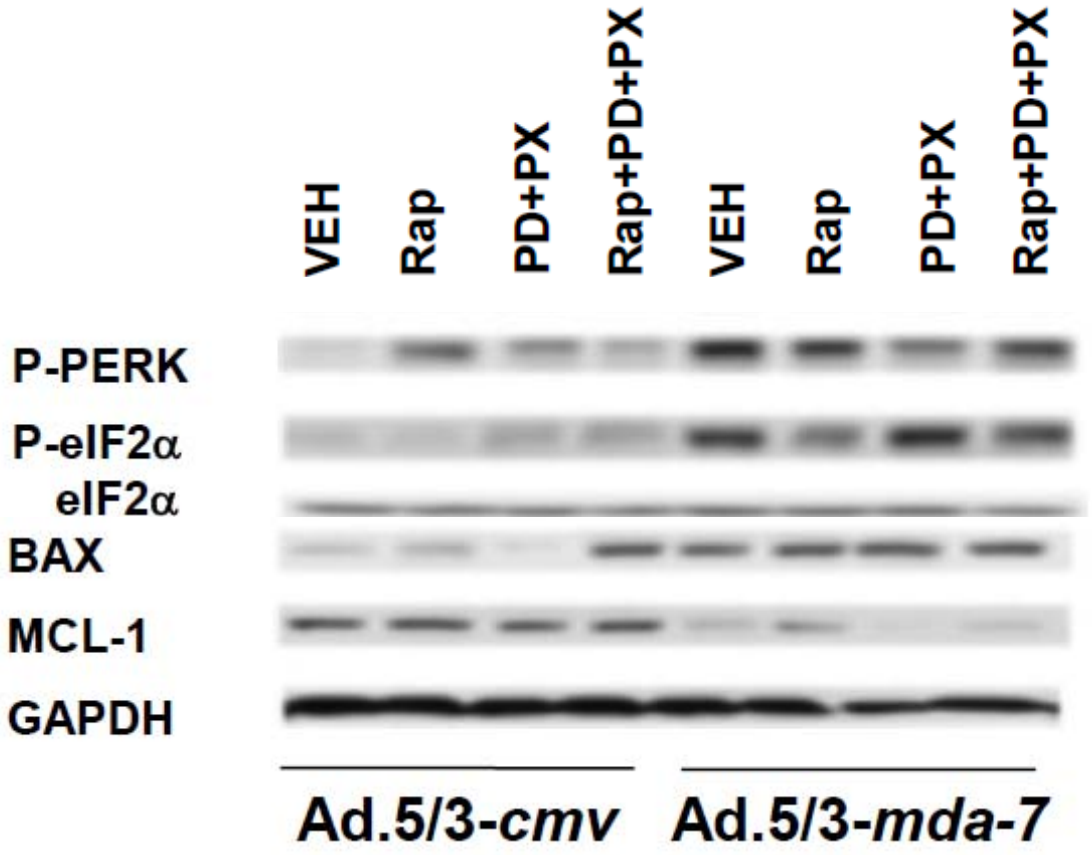

Figure 10: Western blotting confirms ER stress induction by Ad.5/3-*mda-7*. Cells were plated in 60 mm dish (2 x 10^5 cells/dish) and were infected with appropriate adenovirus 24 hrs later. Cells were treated with appropriate small molecule inhibitors 24 hrs after infection, and lysed 6 hrs after treatment. Data are from a representative experiment (n=3). PD=PD184352, PX=PX866, Rap=Rapamycin

Figure 11

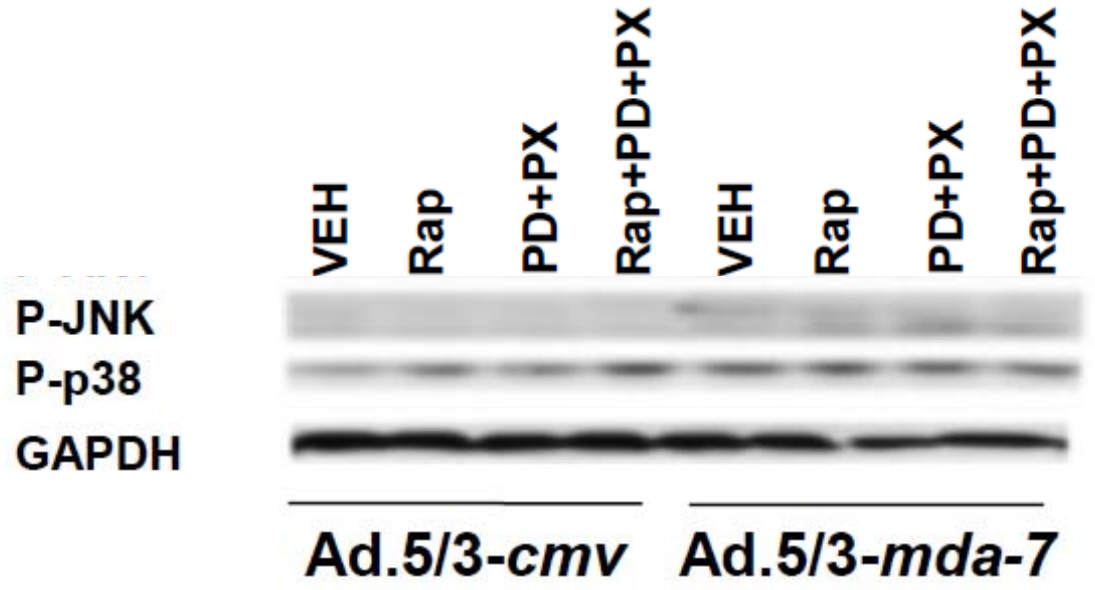

Figure 11: Western blotting confirms upregulation of MAPK signaling by Ad.5/3-*mda-7*. Cells were plated in 60 mm dish (2 x 10^5 cells/dish) and were infected with appropriate adenovirus 24 hrs later. Cells were treated with appropriate small molecule inhibitors 24 hrs after infection, and lysed 6 hrs after treatment. Data are from a representative experiment (n=3). PD=PD184352, PX=PX866, Rap=Rapamycin

Figure 12

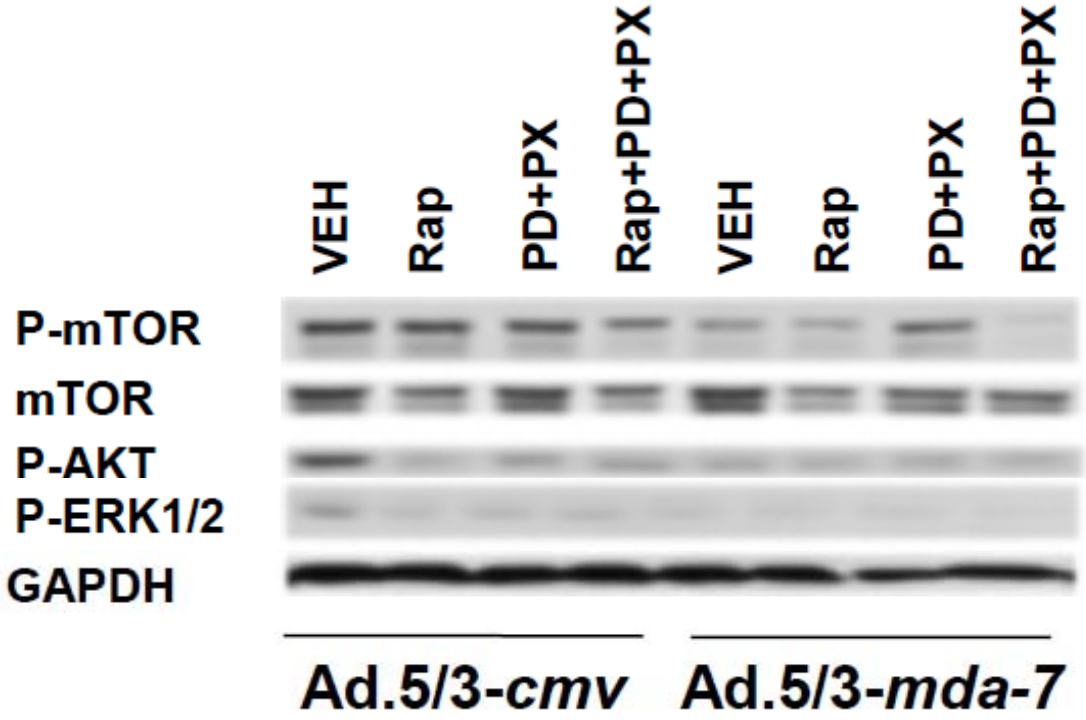

Figure 12: Small molecule inhibitors work to inhibit PI3K pathway. Cells were plated in 60 mm dish (2 x 10^5 cells/dish) and were infected with appropriate adenovirus 24 hrs later. Cells were treated with appropriate small molecule inhibitors 24 hrs after infection, and lysed 6 hrs after treatment. Data are from a representative experiment (n=3). PD=PD184352, PX=PX866, Rap=Rapamycin

CHAPTER FOUR:

DISCUSSION

4.1 Discussion

Renal cell carcinoma has been shown to be resistant to traditional chemotherapy and produce low response rates to current radiation and chemotherapies, including IL-2 and IFN-α (Thompson 2009). Prior to 2005, IL-2 and IFN-α were the only approved systemic therapies for RCC; however these cytokines only provided a clinical benefit for about 15% of RCC patients while causing significant systemic toxicity (Thompson 2009).

The aim of this project was to investigate the response to the novel cytokine MDA-7/IL-24 in RCC, due to its successful application to a wide spectrum of human cancer cells (Fisher 2005). Additionally, this project studied the effect of small molecule inhibitors combined with the adenovirus delivery of *mda-7*. The laboratory work performed throughout this project is designed to be a first step towards a clinical trial with these combinations, and the preliminary data support the transition from the bench to the clinic.

Due to the recent synthesis of Ad.5/3-*mda-7*, expressing MDA-7/IL-24 in the cell has become much easier in cells lacking CAR. Past experiments with Ad.*mda-7* proved to be unable to alter RCC proliferation, which was determined to be the cause of a lack of CAR expression on RCC cells (Yacoub et al. 2003). As was shown in Figure 6 and Figure 7, infection with Ad.5/3-*mda-7* caused greater cell death than infection with Ad.5/3-*cmv* empty vector. The mechanism of action was determined through a series of western blots

showing an upregulation of ER stress proteins coupled with an upregulation of MAPK proteins. This suggests a dual action of MDA-7/IL-24: activation of the ER stress pathway, and upregulation of MAPK pathways leading to cell death.

It was no surprise that RCC cells treated with both Ad.5/3-*mda-7* and small molecule inhibitors would show an increased percentage of cell death; however, the combined effect suggesting a synergy between Ad.5/3-*mda-7* and small molecule inhibitors was not expected. The combinatorial treatment caused a greater percentage cell death than the sum of the two individual treatments. This suggests that there is a significant amount of crosstalk between the MAPK pathways and potentially the PI3K pathway as well.

The complexity of intracellular signaling has long been established. With the mounting number of signaling cascades and kinase pathways it would be unreasonable to presume that each pathway operates discretely. For this reason, crosstalk, or signaling between pathways designed to elicit specific cellular responses, has been recently investigated in MAPK pathways as a potential explanation for decreased cellular growth (Junttila et al. 2008). There is evidence that both p38 signaling and JNK signaling is capable of inhibiting the ERK pathway of cellular growth, which could explain the downregulation of P-ERK in all Ad.5/3-*mda-7* in Figure 12. Crosstalk, combined with the synergy between the treatments that were observed, resulted in an increased percentage of cell death- especially in the Ad.5/3-*mda-7* infection plus PD184352+PX866+Rapamycin treatment.

Although this treatment regimen was successful in killing A498 RCC cells in vitro, the next step would be to try these drug combinations in vivo. If these same drug combinations (Ad.5/3-*mda-7* with PD184352+PX866+Rapamycin) caused a decrease in tumor size in a mouse model, there would be sufficient evidence to warrant a clinical trial with MDA-7/IL-24 and these small molecule inhibitors.

The goal of this project was to explore the ability of Ad.5/3-*mda-7* to successfully infect RCC cells to increase cell death, and to test combinations of small molecule inhibitors to determine the most effective treatment. From the data, it can be concluded that infection with Ad.5/3-*mda-7* and treatment with PD184352+PX866+Rapamycin caused the most cell death in renal cancer cells. This project provides evidence to support an *in vivo* trial, and potentially a clinical trial, due to the possibility that this regimen could be more effective in the treatment of renal cell carcinoma than current therapies.

REFERENCES

Ahmedin J, Siegel R, Ward E, Yongping H, Jiaquan X, Thun M. Cancer Statistics, 2009. *CA: A Cancer Journal for Clinicians*. 2009; 59:225-249.

Bree RT, Stenson-Cox C, Grealy M, Byrnes L, Gorman AM, Samali A. Cellular Longevity: Role of Apoptosis and Replicative Senescence. *Biogerontology*. 2002; 3:195-206.

Bleumer I, Oosterwijk E, De Mulder P, Mulders, P. Immunotherapy for Renal Cell Carcinoma. *European Urology*. 2003; 44: 65-75.

Cersosimo R. Renal cell carcinoma with an emphasis of drug therapy of advanced disease, part 1. *American Journal of Health-System Pharmacy*. 2009; 66(17): 1525-2536.

Chaisuparat R, Hu J, Jham B, Knight Z, Shokat K, Montaner S. Dual Inhibition of PI3Kα and mTOR as an Alternative Treatment for Kaposi's Sarcoma. *Cancer Research.* 2008; 68(20): 8361-8368.

Dash R, Dmitriev I, Su Z, Bhutia S, Azab B, Vozhilla N, Yacoub A, Dent P, Curiel D, Sarkar D, Fisher P. Enhanced Delivery of *mda-7/IL-24* Using a Serotype Chimeric Adenovirus (Ad.5/3) Improves Therapeutic Efficacy in Low CAR Prostate Cancer Cells. *Cancer Gene Therapy*. 2010; in press.

Dent P, Curiel D, Fisher P, Grant S. Synergistic combinations of signaling pathway inhibitors: Mechanisms for improved cancer therapy. *Drug Resistance Updates*. 2009; 12: 65-73.

Emdad L, Lebedeva I, Su Z, Gupta P, Sauane M, Dash R, Grant S, Dent P, Curiel D, Sarkar D, Fisher P. Historical perspective and recent insights into our understanding of the molecular and biochemical basis of the antitumor properties of *mda-7*/IL-24. *Cancer Biology & Therapy*. 2009; 8:5: 391-400.

Erhardt P, Cooper G. Activation of the CPP_{32} Apoptotic Protease by Distinct Signaling Pathways with Differential Sensitivity to Bcl-XL. *The Journal of Biological Chemistry*. 1996; 271(30): 17601-17604.

Fisher P, Gopalkrishnan R, Chada S, Ramesh R, Grimm E, Rosenfeld M, Curiel D, Dent P. *mda-7/IL-24*, A Novel Cancer Selective Apoptosis Inducing Cytokine Gene. *Cancer Biology and Therapy*. 2003; 2(4):Suppl. 1: S23-S37.

Fisher P. Is *mda-7/IL-24* a "Magic Bullet" for Cancer? *Cancer Research*. 2005; 65(22): 10128-10138.

Fulda S, Debatin K-M. Extrinsic versus intrinsic apoptosis pathways in anticancer chemotherapy. *Oncogene*. 2006; 25:4798-4811.

Gao N, Flynn D, Zhang Z, Zhong X, Walker V, Liu K, Shi X, Jiang B. G1 cell cycle progression and the expression of G1 cyclins are regulated by PI3K/AKT/mTOR/p70S6K1 signaing in human ovarian cancer cells. *American Journal of Physiology- Cell Physiology*. 2004; 287: C281-C291.

Hengartner, M. The biochemistry of apoptosis. *Nature*. 2000; 407: 770-776.

Henry-Mowatt J, Dive C, Martinou J, James D. Role of mitochondrial membrane permeabilization in apoptosis and cancer. *Oncogene*. 2004; 23: 2850-2860.

Herrmann E, Bierer S, Wülfing C. Update on systemic therapies of metastatic renal cell carcinoma. *World Journal of Urology*. 2010. Online ahead of print

Hosoi T, Ozawa K. Endoplasmic reticulum stress in disease: mechanisms and therapeutic opportunities. *Clinical Science*. 2010; 118: 19-29.

Ihle N, Williams R, Chow S, Chew W, Berggren M, Pain-Murrieta G, Minion D, Halter R, Wipf P, Abraham R, Kirkpatrick L, Powis G. Molecular pharmacology and antitumor activity of PX-866, a novel inhibitor of phosphoinositide-3-kinase signaling. *Molecular Cancer Therapeutics*. 2004; 3(7): 763-772.

Junttila M, Li S, Westermarck J. Phosphate-mediated crosstalk between MAPK signaling pathways in the regulation of cell survival. *The Federation of American Societies for Experimental Biology Journal.* 2008; 22(4): 954-965.

Kapoor A, Gharajeh A, Sheikh A, Pinthus J. Adjuvant and neoadjuvant small-molecule targeted therapy in high-risk renal cell carcinoma. *Current Oncology.* 2009; 16:1:S60-S66.

Kischkel FC, Hellbardt S, Behrmann I, Germer M, Pawlita M, Krammer PH, Peter ME. Cytotoxicity-dependent APO-1 (Fas/CD95)-associated proteins form a death-inducing signaling complex (DISC) with the receptor. *EMBO J*. 1995; 14(22):5579-5588.

Lavrik I, Golks A, Krammer P. Caspases: Pharmacological Manipulation of Cell Death. *Journal of Clinical Investigation*. 2005; 115(10):2665-2672.

Park M, Walker T, Martin A, Allegood J, Vozhilla N, Emdad L, Sarkar D, Rahmani M, Graf M, Yacoub A, Koumenis C, Spiegel S, Curiel D, Voelke-Johnson C, Grant S, Fisher P, Dent P. MDA-7/IL-24-induced cell killing in malignant renal carcinoma cells occurs by a ceramide/CD95/PERK-dependent mechanism. *Molecular Cancer Therapeutics*. 2009;8(5): 1280-1291.

Rasheva V, Domingos P. Cellular Responses to Endoplasmic Reticulum Stress and Apoptosis. *Apoptosis*. 2009;14(8): 996-1007.

Raynaud F, Eccles S, Clarke P, Hayes A, Nutley B, Alix S, Henley A, Di-Stefano S, Ahmad Z, Guillard S, Bjerke L, Kelland L, Valenti M, Patterson L, Gowan S, Brandon A, Hayakawa M, Kaizawa H, Koizumi T, Ohishi T, Patel S, Saghir N, Parker P, Waterfield M, Workman P. Pharmacologic Characterization of a Potent Inhibitor of Class I Phosphatidylinositide 3-Kinases. *Cancer Research*. 2007; 67(12): 5840-5850.

Saylor PJ, Michaelson MD. New Treatments for Renal Cell Carcinoma: Targeted Therapies. *Journal of the National Comprehensive Cancer Network*. 2009; 7(6): 645-656.

Sebolt-Leopold J, Dudley D, Herrera R, Van Becelaere K, Wiland A, Gowan R, Tecle H, Barrett S, Bridges A, Przybranowski S, Leopold W, Saltiel A. Blockade of the MAP kinase pathways suppresses growth of colon tumors in vivo. *Nature Medicine*. 1999; 5(7): 810-816.

Sehgal S. Sirolimus: Its Discovery, Biological Properties, and Mechanism of Action. *Transplantation Proceedings*. 2003;35(S 3A): 7S-14S.

Thompson, J. Metastatic Renal Cell Carcinoma: Current Standards of Care. 2009; 13:6:S 8-12.

Yacoub A, Mitchell C, Brannon J, Rosenberg E, Qiao L, McKinstry R, Linehan W, Su Z, Sarkar D, Lebedeva I, Valerie K, Gopalkrishnan R, Grant S, Fisher P, Dent P. MDA-7 (Interleukin-24) Inhibits the Proliferation of Renal Carcinoma Cells and Interacts with Free Radicals to Promote Cell Death and Loss of Reproductive Capacity. *Molecular Cancer Therapeutics*. 2003; 2:623-632.

Ziegler U, Groscurth P. Morphological Features of Cell Death. *News in Physiological Science.* 2004; 19:124-128.

VITA

Patrick Eulitt was born on July 24, 1986 in Baltimore, Maryland to Paul and Sherry Eulitt and is an American citizen. He graduated from Mount Hebron High School in Ellicott City, Maryland in May of 2004. He received his Bachelor of Arts in Chemistry from Wake Forest University in Winston-Salem, North Carolina in 2008. He received his Master of Science in Physiology from Virginia Commonwealth University in Richmond, Virginia in April of 2010. In addition to his Masters research in Neuro-Oncology, Patrick has completed research internships at Johns Hopkins University in the Cardiology Department, and Wake Forest University in the Neurology Department.

Publications:

Manuscripts

Hamed HA, Yacoub A, Park MA, **Eulitt P**, Sarkar D, Dimitriev IP, Chen CS, Grant S, Curiel DT, Fisher PB, Dent P. OSU-03012 enhances Ad.mda-7-induced GBM cell killing via ER stress and autophagy and by decreasing expression of mitochondrial protective proteins. Cancer Biology Therapeutics 2010; Apr 4;9(7) (Electronic publication ahead of print)

Hamed HA, Yacoub A, Park MA, **Eulitt PJ,** Dash R, Sarkar D, Dmitriev IP, Lesniak MS, Shah K, Grant S, Curiel DT, Fisher PB, Dent P. Inhibition of Multiple Protective Signaling Pathways and Ad.5/3 Delivery Enhances mda-7/IL-24 Therapy of Malignant Glioma. Molecular Therapy 2010; Feb 23. (Electronic publication ahead of print)

Cartwright M, Brown M, **Eulitt P**, Walker F, Lawson V, Caress J. Diagnostic Nerve Ultrasound in Charcot-Marie-Tooth Type 1B. Muscle and Nerve 2008; Jul;40(1):98-102

Abstracts

Abraham J, **Eulitt P**, Abraham T. The Apex Does Not "Balloon" in Left Ventricular Apical Ballooning Syndrome. Journal of Cardiac Failure 2008; 14(6): 1 S30.

Liang H, **Eulitt P**, Szczesna-Cordary D, Abraham T. High Resolution Echocardiography Indicates Diastolic Dysfunction Without Hypertrophy In A Novel Murine Model of Hypertrophic Cardiomyopathy. Journal of the American College of Cardiology 2007; 49(9): 74A.

Pinheiro A, Liang H, Dimaano L, **Eulitt P**, Corretti M, Schulman S, Abraham T. Abnormal Regional Right Ventricular Mechanics In Acute Myocardial Infarction Without Evidence of Right Ventricular Involvement by Wall Motion Analysis or Electrocardiography. Circulation 2007; 116: II_570.

Liang H, Cheng A, Berger R, Agarwal K, **Eulitt P**, Kass D, Abraham T. Atrial Pacing Induces Atrial Mechanical Dyssynchrony Resulting in Reduced Left Ventricular Performance in Heart Failure Patients On Cardiac Resynchronization Therapy. Journal of the American College of Cardiology 2007; 49(9): 174A.

Conference Presentations:

Abstracts

Pinheiro A*, Dimaano V, **Eulitt P**, Abraham J, Corretti M, Abraham T. Abnormal Regional Right Ventricular Diastolic Mechanics in Hypertrophic Cardiomyopathy Despite Preserved Systolic Mechanics. American Heart Association Scientific Sessions 2008.

Abraham J*, **Eulitt P**, Abraham T. The Apex Does Not "Balloon" in Left Ventricular Apical Ballooning Syndrome. Heart Failure Society of America Annual Scientific Meeting 2008.

Liang H, **Eulitt P***, Szczesna-Cordary D, Abraham T. High Resolution Echocardiography Indicates Diastolic Dysfunction Without Hypertrophy In A Novel Murine Model of Hypertrophic Cardiomyopathy. American College of Cardiology Annual Scientific Session 2007.

Pinheiro A*, Liang H, Dimaano L, **Eulitt P**, Corretti M, Schulman S, Abraham T. Abnormal Regional Right Ventricular Mechanics in Acute Myocardial Infarction Without Evidence of Right Ventricular Involvement by Wall Motion Analysis or Electrocardiography. American Heart Association Scientific Sessions 2007.

Liang H*, Cheng A, Berger R, Agarwal K, **Eulitt P**, Kass D, Abraham T. Atrial Pacing Induces Atrial Mechanical Dyssynchrony Resulting in Reduced Left Ventricular Performance in Heart Failure Patients On Cardiac Resynchronization Therapy. American College of Cardiology Annual Scientific Session 2007.

Abraham T, Liang H, **Eulitt P**, Guzman G, Diaz-Perez Z, Szczesna-Cordary D*. *In Vivo* Examination of Transgenic Mouse Hearts Expressing Familial Hypertrophic Cardiomyopathy Mutations (R58Q and N47K) of Myosin Regulatory Light Chain. Biophysical Society Annual Meeting 2007.

* indicates presenter